Available online at www.sciencedirect.com
ScienceDirect
Solid State Communications 143 (2007) 471–475
solid state communications
www.elsevier.com/locate/ssc

First-principles study of arsenic impurity clusters in molecular beam epitaxy (MBE) grown HgCdTe

He Duan, Xiaoshuang Chen*, Yan Huang, Wei Lu*

National Laboratory for Infrared Physics, Shanghai Institute of Technical Physics, Chinese Academy of Sciences, 200083 Shanghai, China

Received 4 February 2007; received in revised form 21 May 2007; accepted 25 June 2007 by X.C. Shen
Available online 6 July 2007

Abstract

The understanding of the microstructures of the arsenic tetramer (As_t), dimer (As_d), and singlet (As_s) of HgCdTe is important to explain the high electrical compensation of molecular beam epitaxy (MBE) samples and the conversion to *p*-type behavior. The stable configurations were obtained from the first-principles calculations for the arsenic cluster defects [As_n ($n = 1$, 2, and 4)] in as-grown HgCdTe. According to the defect formation energies calculated under Te-rich conditions, the most probable configurations of As_t, As_d, and As_s have been established. For the optimized As_t and As_d the energy is favorable to combine in a nearest neighboring mercury vacancy (V_{Hg}), and the corresponding configurations can be used to explain the self-compensated *n*-type characteristics in as-grown materials. As_t is likely to be more abundant than As_d in as-grown materials, but arsenic atoms are more strongly bounded in As_t than in As_d, thus more substantial activation energy is needed for As_t than that for As_d. The atomic relaxations as well as the structural stability of the arsenic defects have also been investigated.

PACS: 31.15.Ew; 71.15.Mb; 81.15.Hi

Keywords: A. HgCdTe; C. Arsenic incorporation; D. Compensated n-type doping; D. First-principles calculations

1. Introduction

The group V elements are preferred over the mercury vacancies and the group I elements for extrinsic acceptor doping due to their low diffusivity in HgCdTe. Arsenic is a group V element that has received great attention in recent years [1,2]. Although success in achieving *p*-type doping of HgCdTe using arsenic has been reported by several groups [3–7], experimental evidence is not yet available as to the chemical nature of the arsenic impurity.

The *in situ* incorporation of arsenic [8] is routine by MBE, but the observed highly compensated n-type behavior in the as-grown samples has never been satisfactorily explained, except for the model developed by Berding et al. with the suggestion that the (As_{Hg}–V_{Hg}) pair is the culprit [9]. Also, the complete arsenic activation is confined to the arsenic concentration above 10^{16} cm^{-3}, as adopted by many approaches. Otherwise, the arsenic activation appears to be masked by some unidentified *n*-type defects [10]. Unfortunately, the understanding of such defects, which is vital to the control of the arsenic concentration lower than 10^{16} cm^{-3} for high-operating-temperature infrared photodetectors, has not been established. Moreover, an examination of the activated arsenic structures is necessary to confirm the impurity states determined by Hall measurements, especially for the controversial deep acceptor levels [11].

The microscopic behavior of the *in situ* impurity (As_{Hg}) and V_{Hg} has been studied in our previous work [12,13]. With the goal of better understanding the microscopic behavior of arsenic incorporation during MBE growth, we analyzed the properties of the complex defects in the form of arsenic tetramer, dimer, and singlet in the present work. We calculated the formation energies of possible configurations for As_n ($n = 1$, 2, and 4), from which the stable configurations were obtained.

2. Computational methods

In our calculations, we chose HgTe as the host system. The random-distributions of cation atoms in HgCdTe system

* Corresponding author.
E-mail addresses: xschen@mail.sitp.ac.cn (X. Chen), luwei@mail.sitp.ac.cn (W. Lu).

0038-1098/$ - see front matter © 2007 Elsevier Ltd. All rights reserved.
doi:10.1016/j.ssc.2007.06.032

is not in consideration in this design. The choice of HgTe is feasible because of the equivalent properties between HgTe and technologically important HgCdTe with low Cd fraction. The total energy calculations were performed within the generalized-gradient approximation (GGA) implemented by the plane-wave total energy VASP code [14] with the Vanderbilt ultrasoft pseudopotentials [15]. The cutoff energy for the wave functions was 280 eV. The calculated ground lattice constant for bulk HgTe was 6.66 Å, in agreement with the experimental value 6.46 Å [16]. We used a 64-atom supercell and a $9 \times 9 \times 9$ k-points Monkhorst-pack mesh in the Brillouin zone of the supercell. All internal structural parameters were fully relaxed until the Hellmann–Feynman (HF) forces were converged to within 0.1 meV/Å. The defect system was modeled by putting a complex defect at the center of a periodic supercell of HgTe, and all the defect structures considered here are electronically neutral.

3. Results and discussion

3.1. Chemical potential dependence of the formation energy

The formation energies of the defect system were calculated from the total energies based on the standard formalism by Zhang and Northrup [17]. For neutral defect α ($q = 0$) in HgTe, the formation energy ΔH_f ($\alpha, q = 0$) depends on the chemical potential μ_i (i refers to Hg, Te, and As).

$$\Delta H_f(\alpha, q = 0) = \Delta E(\alpha, q = 0) + n_{\mathrm{Hg}}\mu_{\mathrm{Hg}} + n_{\mathrm{Te}}\mu_{\mathrm{Te}} + n_{\mathrm{As}}\mu_{\mathrm{As}} \quad (1)$$

where

$$\Delta E(\alpha, q = 0) = E_{\mathrm{tot}}(\alpha, q = 0) - E_{\mathrm{tot}}(\mathrm{HgTe}) + n_{\mathrm{Hg}}\mu^0_{\mathrm{Hg}} + n_{\mathrm{Te}}\mu^0_{\mathrm{Te}} + n_{\mathrm{As}}\mu^0_{\mathrm{As}}. \quad (2)$$

Here, E_{tot} (α, $q = 0$) is the total energy for the defective supercell, E_{tot} (HgTe) is the total energy for the same supercell in the absence of α, the n_i is the number of Hg, Te, and As atoms transferred from the supercell to the reservoirs in forming the defect, respectively, μ_i is the chemical potential referenced to elemental liquid/solid with energy μ^0_i. However, the achievable values of μ_i are limited thermodynamically under equilibrium growth conditions. First, to avoid precipitation of the constituent i, μ_i is bound by

$$\mu_{\mathrm{Hg}} < 0, \quad \mu_{\mathrm{Te}} < 0, \quad \mu_{\mathrm{As}} < 0. \quad (3)$$

Second, to maintain a stable HgTe compound, μ_i is bound by

$$\mu_{\mathrm{Hg}} + \mu_{\mathrm{Te}} = \Delta H_f(\mathrm{HgTe}). \quad (4)$$

The calculated ΔH_f (HgTe) is -3.65 eV, in agreement with the experimental value -3.3 eV [18]. Finally, to avoid the formation of secondary phases As_2Te_3, μ_i is bound by

$$2\mu_{\mathrm{As}} + 3\mu_{\mathrm{Te}} < \Delta H_f(\mathrm{As_2Te_3}). \quad (5)$$

Fig. 1 plots the accessible chemical potential region for HgTe:As, as defined by Eqs. (3)–(5). It is shown that because arsenic and tellurium form a very stable compound As_2Te_3 with a rather low formation energy -8.65 eV, the highest possible μ_{As}, at the Hg-rich condition ($\mu_{\mathrm{Hg}} = 0$, $\mu_{\mathrm{Te}} = -3.65$ eV), is -3.85 eV. Under the Te-rich condition ($\mu_{\mathrm{Hg}} = -3.65$ eV, $\mu_{\mathrm{Te}} = 0$), μ_{As} is further reduced to less than -9.33 eV. Above these chemical potential limits, secondary As_2Te_3 compound will be formed, thus stopping the arsenic doping process. Such low accessible μ_{As} is one of the limiting factors for arsenic doping in HgCdTe.

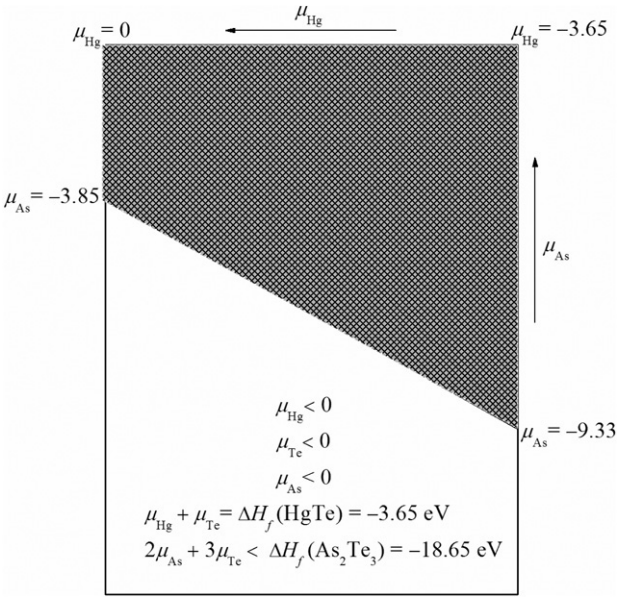

Fig. 1. Calculated accessible equilibrium chemical potential region for HgTe doped with arsenic in the two-dimensional (μ_{Hg}, μ_{As}) plane. The shaded area is forbidden under equilibrium growth conditions.

3.2. Possible configurations for the complex defects As_n (n = 1, 2, and 4)

3.2.1. Arsenic tetramers

Under Te-saturated condition, the density of V_{Hg} is much higher than that of tellurium vacancy (V_{Te}), so that the As_4 defects with two of the four arsenic atoms occupying mercury sites are expected to be the most reasonable configuration. In our calculations, we typified such As_4 defects into arsenic tetramers (As_t) and isolated arsenic atoms (4As), respectively (see Fig. 2).

As_t can be regarded as the distorted pyramidal structure of As_4 molecules. During typical low-temperature MBE growth, there are difficulties in cracking As_4 into As_2 or As_1 on the growing surface, so that As_4 molecules initially absorbed on the surface are subjected to the stress exerted by the HgTe lattice owing to the different properties of the dopant and host atoms. The stress can be released at the cost of the break of the partial As–As bonds. In this way the pyramidal structure distorts into the tetramer configuration. For As_t shown in Fig. 2 the optimized As–As split changes from 2.45 Å for configuration (c) to 2.555 Å for configuration (a), approximately conserving the experimental value 2.435 Å for the pyramidial As_4 molecular [19].

One can also see that different occupation patterns for As_t produces the dissimilar numbers of the broken As–As bonds

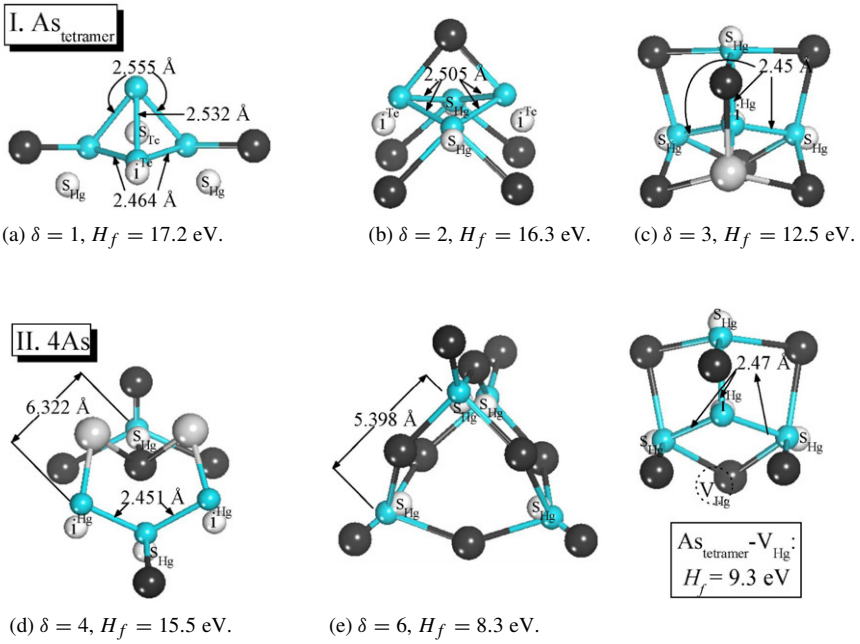

(a) $\delta = 1$, $H_f = 17.2$ eV. (b) $\delta = 2$, $H_f = 16.3$ eV. (c) $\delta = 3$, $H_f = 12.5$ eV.

(d) $\delta = 4$, $H_f = 15.5$ eV. (e) $\delta = 6$, $H_f = 8.3$ eV.

Fig. 2. Calculated ground geometries for the As_4 defects in HgTe, with two of the four arsenic atoms occupying the Hg sites. In this figure, the Hg atoms are of the largest size (in light grey), the Te atoms of intermediate size (in black), and the As atoms are the smallest (in cyan). To analyze the atomic displacements, the As atoms in the pre-relaxed structures are also shown by the smallest atoms (in white). For the labels on the As atoms, "s" and "i" denotes the substitutional site and the interstitial site, respectively. (For interpretation of the references to colour in this figure legend, the reader is referred to the web version of this article.)

(designated as δ), and the values of δ for all the possible As_t defects do not exceed 3 ($\delta \leq 3$). This can be understood from the bondlength of 2.435 Å for the pyramidial structure, slightly less than the Hg–Te distance of 2.798 Å but far less than the spacing of the nearest neighboring Hg atoms in HgTe (4.57 Å). As a result, As_{Hg}–As_{Hg} bond is to be broken up while the As_{Hg}–As_{Te} bond is left to adjust itself to accommodate the host lattice. In the same way it is conjecturable that the more As_{Hg} units in the As_4 defects leads to the larger value of δ. Fig. 2 also gives the calculated formation energies of the As_4 defects at the Te-rich limit. In the case of As_t the configuration (a) and (b) are metastable states from the formation energies, and the configuration (c) is the most probable one. Therefore, under the equilibrium stage the former two configurations are to be converted into the latter one by means of extra V_{Hg} to release the lattice stress. The geometry of the configuration (c), optimized in a manner of $[(As_{Hg}–As_i)_d]_3$ copolymer (dimer denoted as "*d*"), is not only more favorable in energy by 2 eV lower than the strongest configuration (b), but also stronger with 25% gain in the binding energy with respect to the quasi-pyramidal configuration (a).

When the As–As bonds for As_4 molecular are broken completely ($\delta = 6$) or partially ($3 < \delta < 6$), the perfect pyramidal dissociates into isolated atoms and/or dimers, as demonstrated by the configurations of type II in Fig. 2. Such a situation occurs only under high-temperature growth conditions, which is not applied for the state-of-the-art MBE.

Focusing on the configuration (c), one can see that the atomic relaxation makes the three As_{Hg} atoms to move towards the common As_i atom by an amplitude of 0.348 Å, which leads to the final optimized geometry in $[(As_{Hg}–As_i)_d]_3$ copolymer configuration. However, such a configuration fails to explain the experimental observation of the slight *n*-type conduction in as-grown materials because of the three As_{Hg} atoms with strong donor characteristics. The previous study [20] has given a reasonable explanation of the As_{Hg}–V_{Hg} pairs, suggesting that the behavior of the compensation conduction in as-grown samples is possibly associated with V_{Hg} which is bound to the donor-like arsenic defects. To augment our understanding of such a suggestion, we computed the complex defect of As_t–V_{Hg} (see the last section in Fig. 2), which was modeled by placing an additional V_{Hg} to the given As_t in the configuration (c). The calculated ground geometry of As_t–V_{Hg} displays that the configuration of $[(As_{Hg}–As_i)_d]_3$ is stable, without experiencing the relaxation to other configurations with the perturbation of V_{Hg}. However, the complex defect of $[(As_{Hg}–As_i)_d]_3$–V_{Hg} is found to substantially lower the formation energy $[(As_{Hg}–As_i)_d]_3$ by about 3 eV. This reduction of the formation energy is attributed to the removing of Hg atoms from the defect system, thus effectively compensating the energy lost by the introduction of As atoms into the defect system. Also, the configuration information of the complex defect of $[(As_{Hg}–As_i)_d]_3$–V_{Hg} is deemed to be in analogy to that of clusters of As_{Hg}–V_{Hg} pairs with one common V_{Hg}, so that both of them are of compensating donor nature, as supported by our calculated transition energies (unpublished).

3.2.2. *Arsenic dimer* (As_d) *and singlet* (As_s)

The calculations of As_d and As_s are based on the fact that these defects in a small quality are present in a noncracking arsenic source but predominant in a cracking arsenic source. In Fig. 3(a), we give the probable configuration of As_d

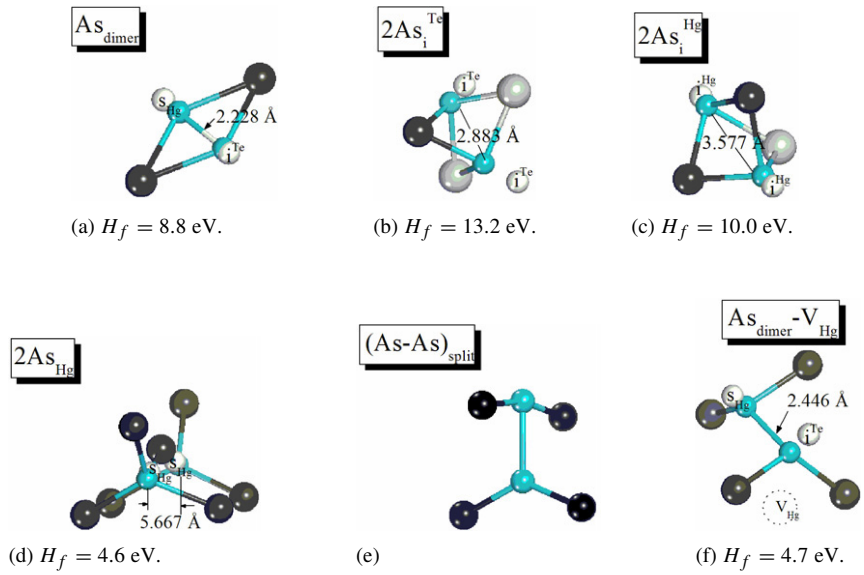

(a) $H_f = 8.8$ eV. (b) $H_f = 13.2$ eV. (c) $H_f = 10.0$ eV.

(d) $H_f = 4.6$ eV. (e) (f) $H_f = 4.7$ eV.

Fig. 3. Calculated ground geometries for As_2 defects in HgTe. The configuration of $(As–As)_{split}$ is assumed to be more plausible than other ones for As_d. The atomic notations are the same as denoted in Fig. 2.

with the lower formation energy. The As–As spacing is 2.228 Å, in agreement with the experimental value 2.10 Å for As_2 molecular [19]. We note that the As_{Hg} atom deviates significantly from the ideal lattice sites toward the interstitial site by an amplitude of 0.783 Å, which suggests that the interstitial sites are favorable in energy to the absorption of As_2 molecules. However, our calculations indicate that two arsenic atoms, both residing in the interstitial sites, can never be configured in As_d unless an amount of energy barriers are overcome when an extra V_{Hg} is available; otherwise, they are in the configuration of two isolated arsenic atoms (2As), as shown in Figs. 3(b) and (c). So the configuration with two arsenic atoms of split interstitial is expected to be the most probable for As_d, but this assumption needs to be examined in our further work. At the same time, we have modeled the complex defect $(As_{Hg}–As_i)_d–V_{Hg}$, as demonstrated by the configuration (f) in Fig. 3. An obvious shift of As_i toward V_{Hg} can be observed, and the amplitude of the As_i relaxation is more significant relative to the $(As_{Hg}–As_i)_d$ defect.

The displacements of As_s are negligible during the atomic relaxations. The lattice relaxation energies are of the order of meV. During the short-displacement and successive-steps of the relaxations, the work done by the HF force can be approximated to that by the first (1) and second (2) nearest neighbors of impurity while the contribution from the more distant neighbors is not taken into account.

$$W^{\mathrm{HF}} = W_1^{\mathrm{HF}} + W_2^{\mathrm{HF}} = \left(\sum F_{i0}^{\mathrm{HF}} \cdot \Delta d_{i0} + \sum F_{ij}^{\mathrm{HF}} \cdot \Delta d_{ij}\right) \Big/ 2. \quad (6)$$

Table 1 displays the evaluation of the work done by the HF force together with the relaxation energies $\Delta E_{\mathrm{relax}}$. One can see that the sum of W_1^{HF} and W_2^{HF} is comparable to the value of $\Delta E_{\mathrm{relax}}$, and the main contributions of the work done by the HF forces come from the second-nearest neighbors.

Table 1
Work of the Hellmann–Feynman forces (HF) (in meV) for the first (1) and second (2) nearest neighbors as well the lattice relaxation energies $\Delta E_{\mathrm{relax}}$ (in meV)

$(\alpha, q = 0)$	W_1^{HF}	W_2^{HF}	$\Delta E_{\mathrm{relax}}$
As_{Hg}	1.68	15.84	19.58
As_{Te}	143.96	530.24	709.67
As_i^{Hg}	27.76	92.13	339.97
As_i^{Te}	3.54	90.76	366.81

3.3. Comparison of the formation energies for As_n ($n = 1$, 2, and 4)

In Fig. 4 we compare the formation energies per arsenic atom for various types of the arsenic defects As_n ($n = 1$, 2, and 4). It can be seen that As_t is more favorable in energy than As_d and As_s, indicating that As_t is more abundant than As_d and As_s in as-grown materials. The order of the formation energies is relevant to the atomic site configurations in arsenic defects, for example, the energy levels of the arsenic defects containing the As_{Te} atoms are much higher than those containing the As_{Hg} atoms. This is a direct effect of the chemical potentials on the formation energies. Under Te-rich condition ($\mu_{Te} = 0$ and $\mu_{Hg} < 0$), more Hg atoms involved in the given defect results in the lower energy levels. From the formation energies of As_n the values of the binding energies are also obtained for As_t and As_d. We find that the more stable configuration corresponds to the stronger binding of the arsenic atoms in As_t and As_d. Since the distorted pyramidal structure of As_4 molecular relieves the lattice stress during MBE growth, the heavier degree of the distortion yields more amount of the lattice stress to be released

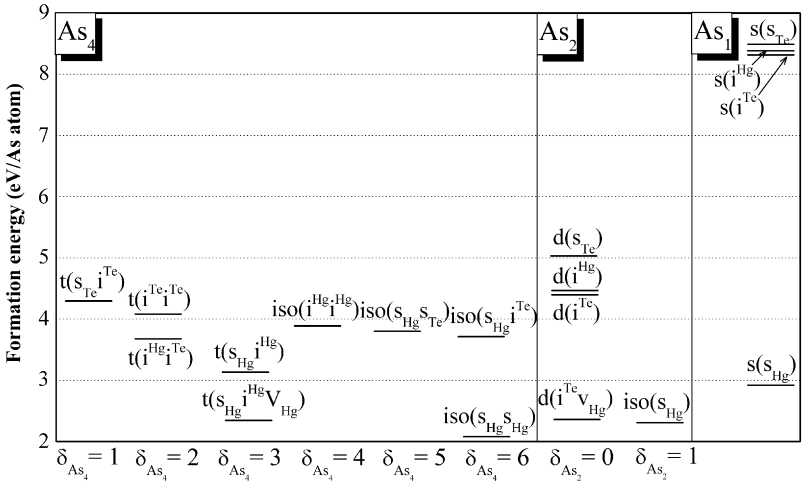

Fig. 4. The comparison of the formation energies per arsenic atom for various types of the As_n ($n = 1$, 2, and 4) defects, evaluated from Eqs. (1)–(3). In the case of the As_4 and As_2 defects, the designated As_{Hg} atoms are omitted in this figure, and the defects of As_t and As_d are simply designated by the remaining two and one arsenic atom(s), respectively.

and thus more steady configurations as well. Moreover, it can be concluded that under thermal equilibrium isolated arsenic atoms prefer to be bound into two or four nearest neighboring atoms, because the binding energies of 2As and 4As defects are at least 0.61 eV/As atom and 0.84 eV/As atom higher than the substitutional singlet (As_{Hg}), respectively.

4. Summary

In summary, we have performed the theoretical calculations for arsenic tetramer (As_t), arsenic dimer (As_d), and arsenic singlet (As_s) in HgCdTe system based on the first-principles calculations. We calculated the defect formation energies from the total-energy calculations, thereby the most probable configurations in the form of $[(As_{Hg}–As_i)_d]_3$ for As_t, $(As_{Hg}–As_i)_d$ for As_d, and As_{Hg} for As_s have been established under Te-rich conditions. In the case of $[(As_{Hg}–As_i)_d]_3$ and As_{Hg}, they are favorable in energy to combine a nearest neighboring V_{Hg}, and the corresponding $[(As_{Hg}–As_i)_d]_3–V_{Hg}$ and $As_{Hg}–As_{Hg}$ defects are thought to explain the self-compensated n-type characteristics in as-grown materials. The absorption of As_2 molecules is assumed to be relevant to the complex defect of $(As–As)_{split}$ instead of $(As_{Hg}–As_i)_d$ because the interstitial sites seem to be preferable. Further studies of the arsenic defects in charge state are necessary to deeply understand the microscopic behavior of arsenic incorporation in HgCdTe.

Acknowledgments

This work was financially supported by the Chinese National Key Basic Research Special Fund, the Key Fund of the Chinese National Science Foundations (No. 10234040), the Chinese National Science Foundations (No. 60221502 and 60476040), and the Key Foundation of Shanghai Commission of Science and Technology (No. 02DJ14006), the Creative Foundation of Shanghai Institute of Technical Physics (No. C2-5). We are also grateful to the Shanghai Super-computer Center.

References

[1] T.C. Harman, J. Electron. Mater. 8 (1989) 191.
[2] P.S. Wijewarnasuriya, S. Sivananthan, Appl. Phys. Lett. 72 (1998) 1694.
[3] M.J. Bevan, M.C. Chen, H.D. Shih, Appl. Phys. Lett. 67 (1995) 3450.
[4] F. Aqariden, P.S. Wijewarnasuriya, S. Sivananthan, J. Vac. Sci. Technol. B 16 (1998) 1309.
[5] L.O. Bubulac, D.D. Edwall, C.R. Wiswanathan, J. Vac. Sci. Technol. B 9 (1991) 1695.
[6] F. Aqariden, H.D. Shih, M.A. Kinch, H.F. Schaake, Appl. Phys. Lett. 78 (2001) 3481.
[7] Y. Selamet, G. Badano, C.H. Grein, P. Boieriu, V. Nathan, S. Sivananthan, Proceedings of SPIE 4454 (2001) 71.
[8] T.S. Lee, J. Garland, C.H. Grein, M. Sumstine, A. Jandeska, Y. Selamet, S. Sivananthan, J. Electron. Mater. 29 (2000) 869.
[9] M.A. Berdinbg, A. Sher, M. Vanschilfgaarde, A.C. Chen, J. Arias, J. Electron. Mater. 27 (1998) 605.
[10] P. Boieriu, C.H. Grein, H.S. Jung, J. Garland, Appl. Phys. Lett. 86 (2005) 212106.
[11] X.H. Shi, S. Rujirawat, R. Ashokan, C.H. Grein, S. Sivananthan, Appl. Phys. Lett. 73 (1998) 638.
[12] L.Z. Sun, X.S. Chen, Y.L. Sun, X.H. Zhou, Zh.J. Quan, H. Duan, W. Lu, Phys. Rev. B 71 (2005) 193203.
[13] L.Z. Sun, X.S. Chen, Y.L. Sun, X.H. Zhou, Zh.J. Quan, H. Duan, W. Lu, Phys. Rev. B 73 (2006) 195206.
[14] G. Kresse, J. Hafner, Phys. Rev. B 47 (1993) 558.
[15] D. Vanderbilt, Phys. Rev. B 41 (1990) 7892.
[16] X.J. Chen, X.L. Hua, J.S. Hu, J.-M. Langlois, W.A. Goddard III, Phys. Rev. B 53 (1996) 1377.
[17] S.B. Zhang, John E. Northrup, Phys. Rev. Lett. 67 (1991) 2339.
[18] M.A. Berding, M. Vanschilfgaarde, A. Sher, J. Electron. Mater. 22 (1993) 1005.
[19] K. Hedberg, Trans. Am. Crystallogr. Assoc. 2 (1966) 79.
[20] M.A. Berding, A. Sher, Appl. Phys. Lett. 74 (1999) 685.